# Site-Directed Mutation of the Highly Conserved Region near the Q-Loop of the Cytochrome *bd* Quinol Oxidase from *Escherichia coli* Specifically Perturbs Heme $b_{595}$†

Jie Zhang,‡ Petra Hellwig,§ Jeffrey P. Osborne,|| Hong-wei Huang,⊥ Pierre Moënne-Loccoz,⊥ Alexander A. Konstantinov,# and Robert B. Gennis*,‡

*Department of Biochemistry, University of Illinois at Urbana-Champaign, 600 South Mathews Avenue, Urbana, Illinois 61801, Department of Biochemistry, Molecular Biology, and Biophysics, University of Minnesota, St. Paul, Minnesota 55108, Institut für Biophysik der Johann-Wolfgang-Goethe-Universität, Theodor-Stern-Kai 7 Haus 74, 60590 Frankfurt am Main, Germany, Department of Biochemistry and Molecular Biology, Oregon Graduate Institute of Science & Technology, 20000 Northwest Walker Road, Beaverton, Oregon 97006, and A. N. Belozersky Institute of Physico-Chemical Biology, Moscow State University, Moscow 119899, Russia*

*Received March 7, 2001; Revised Manuscript Received May 24, 2001*

ABSTRACT: Cytochrome *bd* is one of the two quinol oxidases in the respiratory chain of *Escherichia coli*. The enzyme contains three heme prosthetic groups. The dioxygen binding site is heme *d*, which is thought to be part of the heme−heme binuclear center along with heme $b_{595}$, which is a high- spin heme whose function is not known. Protein sequence alignments [Osborne, J. P., and Gennis, R. B. (1999) *Biochim. Biophys Acta 1410*, 32−50] of cytochrome *bd* quinol oxidase sequences from different microorganisms have revealed a highly conserved sequence (**GW**XXXEX**GR**Q**PW**; bold letters indicate strictly conserved residues) predicted to be on the periplasmic side of the membrane between transmembrane helices 8 and 9 in subunit I. The functional importance of this region is investigated in the current work by site-directed mutagenesis. Several mutations in this region (W441A, E445A/Q, R448A, Q449A, and W451A) resulted in a catalytically inactive enzyme with abnormal UV−vis spectra. E445A was selected for detailed analysis because of the absence of the absorption bands from heme $b_{595}$. Detailed spectroscopic and chemical analyses, indeed, show that one of the three heme prosthetic groups in the enzyme, heme $b_{595}$, is specifically perturbed and mostly missing from this mutant. Surprisingly, heme *d*, while known to interact with heme $b_{595}$, appears relatively unperturbed, whereas the low-spin heme $b_{558}$ shows some modification. This is the first report of a mutation that specifically affects the binding site of heme $b_{595}$.

Cytochrome *bd* quinol oxidase is one of two quinol oxidases in the respiratory chain of *Escherichia coli* (*1*) and is expressed under microaerophilic growth conditions (*2*−*4*). The enzyme is an integral membrane heterodimer (*5*, *6*), and it catalyzes the two-electron oxidation of ubiquinol-8 and the four-electron reduction of dioxygen to water with the release of protons into the periplasmic space and the generation of a protonmotive force (*7*−*9*). Cytochrome *bd* is the only prokaryotic respiratory oxidase that does not belong to the heme−copper oxidase superfamily (*10*, *11*) and shows no homology to the members of this superfamily (*12*, *13*). Cytochrome *bd* contains no copper and does not function as a transmembrane proton pump (*14*), which are both characteristics of the heme−copper oxidases. The enzyme contains three heme prosthetic groups (*15*). Heme $b_{558}$ is a low-spin protoheme IX and is believed to be the initial electron acceptor from ubiquinol (*16*). Reduced heme $b_{558}$ has absorption peaks at 560, 530, and 430 nm. Heme $b_{595}$ is a high-spin protoheme IX, with absorption peaks at 595 and 560 nm and a recently characterized peak (*17*, *18*) at about 440 nm in the reduced state. The role of heme $b_{595}$ is not known. Heme *d* is a high-spin chlorin with an α-absorption band at 628 nm and an uncharacterized Soret peak. Heme $b_{595}$ and heme *d* have been proposed to be in close proximity and to form a diheme binuclear center where oxygen is reduced to water (*18*, *19*).

Recent alignments (*20*) (Figure 1) of the many newly available cytochrome *bd* protein sequences from different bacterial species revealed for the first time a high conserved sequence, (440)**GW**XXXEX**GR**Q**PW**(451) (*E. coli* numbering; bold letters indicate strictly conserved residues), in subunit I, predicted to be on the periplasmic side of the membrane. The importance of this highly conserved region is here examined by site-directed mutagenesis. Six mutants were made: W441A, E445A/Q, R448A, Q449A, and W451A. With the exception of Q449A, all of the mutants are nonfunctional and cannot support aerobic growth. One

† This work was supported by grants from the U.S. Public Health Service, National Institutes of Health, HL16101 (R.B.G.) and GM34468 (to Prof. Thomas M. Loehr), and a Fogarty International Collaboration Award (R.B.G. and A.A.K.); the Howard Hughes Medical Institute (A.A.K.); International Research Scholar Grant 55000320 (A.A.K.); and CRDF Grant (R.B.G. and A.A.K.).

* To whom correspondence should be addressed. Tel: 217-333-9075. Fax: 217-244-3186. E-mail: r-gennis@uiuc.edu.

‡ University of Illinois at Urbana-Champaign.

§ Institut für Biophysik der Johann-Wolfgang-Goethe-Universität.

|| University of Minnesota.

⊥ Oregon Graduate Institute of Science & Technology.

# Moscow State University.

10.1021/bi010469m CCC: $20.00 
Published on Web 06/23/2001

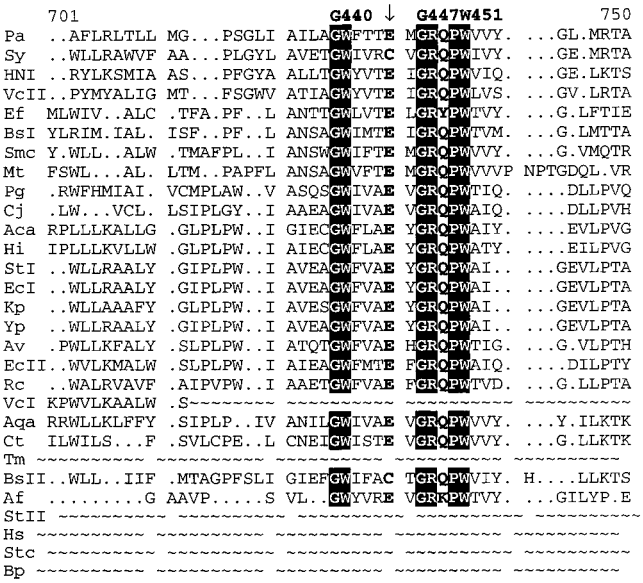


FIGURE 1: Protein sequence alignment of cytochrome *bd* quinol oxidase subunit I showing the conserved region. See ref *20* for details. Highlighted letters are 100% conserved, and bold letters are highly conserved residues. The asterisk (∗) indicates the sequence of the cytochrome *bd* quinol oxidase I from *E. coli*, and the arrow (↓) indicates the highly conserved E445 residue examined in this work.

of the mutants, E445A, was characterized in detail, and the results show that, in this mutant, one of the heme prosthetic groups, heme $b_{595}$, is greatly perturbed and is essentially missing from most preparations of the mutant enzyme. In contrast, heme $b_{558}$ and heme *d* are not grossly perturbed. This is particularly surprising given the indications that heme $b_{595}$ and heme *d* are in close proximity (*21*−*24*). Hence, mutations in this region of the protein may be of great help in studying the role of heme $b_{595}$ in the catalytic mechanism. In this paper, the characterization of the E445A mutant is described using UV−vis, electron paramagnetic resonance (EPR),[1] FTIR, and resonance Raman spectroscopies, as well as electrochemical measurements.

## MATERIALS AND METHODS

*Strains and Plasmids*. *E. coli* strain GO105 (*cyd AB::kan, cyo, recA*), which lacks both cytochrome $bo_3$ and cytochrome *bd* quinol oxidases (*25*), was used as the host strain for expressing both the wild-type and mutant cytochrome *bd* on a plasmid. Under the selection conditions utilized, the second cytochrome *bd* oxidase (*bd*-II), encoded by the *E. coli app* operon (*26*), is not expressed. To obtain wild-type cytochrome *bd*, plasmid pTK1 (*25*) was introduced to the strain. This plasmid is a derivative of pBR322 and contains the whole operon encoding wild-type cytochrome *bd* as well as the ampicillin-resistance gene for selection. Mutants of cytochrome *bd* were also expressed using this same plasmid system.

*Site-Directed Mutagenesis and Complementation Analysis.* The Stratagene QuikChange mutagenesis kit was used to construct mutants using pTK1 as the template (*25*). The protocol followed was described in ref *27*. All mutations were confirmed by DNA sequencing. The complementation test was carried out as follows. Plasmid DNA from mutants was used to transform GO105 using the TSS method (*28*). Cells were grown anaerobically, selecting of ampicillin resistance. The strains exhibiting ampicillin resistance were restreaked to obtain single colonies and then were grown aerobically on M63 (*29*) minimal plates supplemented with 0.3% lactate and 0.3% succinate, plus 100 $\mu$g/mL ampicillin and 50 $\mu$g /mL kanamycin. Complementation was defined by the appearance of colonies within 48−72 h of incubation at 37 °C.

*Cell Growth and Preparation of Protein Samples*. Large-scale cell growth was carried out at the Fermentation Facility at the University of Illinois at 37 °C, pH 7, in a 200 L fermenter (for GO105/pTK1/E445A and GO105/pTK1) or a 20 L fermenter (for GO105 with all other noncomplementing mutants). LB medium with 0.3% glucose, and antibiotics were used for growth. Both wild-type and the E445A mutant cytochrome *bd* oxidases were purified from isolated membranes of GO105/pTK1 as described previously (*8*), except that the hydroxyapatite column was omitted. Fractions with an $A_{412}/A_{280}$ ratio greater than 0.5 were collected from a Fast-Flow Sepharose DEAE column. The pooled fractions were concentrated to the desired concentration using an Amicon concentrator with a 50 kDa filter and then dialyzed three times against 50 mM sodium phosphate buffer, pH 7.9, containing 5 mM EDTA and 0.05% *N*-lauroylsarcosine (sodium salt). Both wild-type and mutant cytochrome *bd* samples were then examined, using the same dialysis buffer for appropriate dilutions unless specified otherwise.

*Ubiquinol-1 and TMPD Oxidase Activity Assays*. Cytochrome *bd* mutants were assayed both in isolated membranes, in which there is no other quinol oxidase, and with the purified enzyme. For membranes, samples were homogenized in 25 mM Tris-HCl and 1 mM EDTA, pH 7.5. Purified protein samples were dialyzed against 50 mM sodium phosphate buffer, pH 7.9, containing 5 mM EDTA and 0.05% *N*-lauroylsarcosine (sodium salt). Various dilutions of either the homogenized membrane samples or pure protein samples were added to 1.9 mL of the respective buffer containing either 2 mM dithiothreitol or 4 mM ascorbate that had been equilibrated to 37 °C in a Clark-type oxygen electrode (Yellow Springs Instrument Co.). A baseline was taken, and the reaction was initiated by addition of ubiquinol-1 (kindly provided by Hoffman-LaRoche) or TMPD to a final concentration of 245 $\mu$M and 1 mM, respectively. Activities were determined assuming a value of 237 $\mu$M $O_2$ for air-saturated buffer at 37 °C.

*Optical Spectroscopic Measurements*. All of the absorbance spectra in the UV−vis region were obtained with a DW2000 spectrophotometer (Aminco) using a 1 cm pathlength cuvette. The series of absorbance spectra used to determine the heme midpoint potentials were obtained with a UV-2101PC scanning spectrophotometer (Shimadzu).

*Heme Analysis*. The heme *b* contents of both wild-type and E445A mutant purified cytochrome *bd* were measured by the pyridine hemochromogen assay, using an extinction coefficient for the wavelength pair 556.5−540 nm = 23.98 $mM^{-1}$ $cm^{-1}$ (*30*). The heme *d* content was determined from

[1] Abbreviations: BCA, bicinchoninic acid; DAD, diaminodurene; DTT, dithiothreitol; EDTA, ethylenediaminetetraacetic acid; $E_m$, midpoint potential; EPR, electron paramagnetic resonance; FTIR, Fourier transform infrared; LB, Luria broth; TMPD, tetramethylphenylenediamine; UQ-1/$UQH_2$-1, ubiquinone-1/ubiquinol-1; WT, wild type; RR, resonance Raman.

Table 1: Summary of the Characteristics of Mutants in Subunit I of Cytochrome *bd*[a]

| | complementation analysis | ubiquinol-1 oxidase activity (% of wild type) | TMPD oxidase activity (% of wild type) | heme content ($\mu$mol of heme *b*/ $\mu$mol of heme *d*) | UV−vis spectral features |
|---|---|---|---|---|---|
| wild type | + | 100 | 100 | 2.06 | WT spectra |
| E445A mutant | − | 0.2 | 0.7 | 1.18 ± 0.33 | no heme $b_{595}$ absorbance bands |
| E445Q mutant[b] | − | 1.2 | 2.9 | nd[c] | no heme $b_{595}$ absorbance bands |
| W441A mutant | − | nd | nd | nd | nd |
| R448A mutant[b] | − | | | nd | decreased heme *d* band |
| Q449A mutant | + | 100 | 100 | nd | WT spectra |
| W451A mutant | − | nd | nd | nd | nd |

[a] Assays were conducted with purified enzymes unless otherwise indicated. [b] Evaluated using membrane preparations. [c] nd, not determined.

the reduced *minus* "as isolated" difference spectrum with the $\Delta\epsilon$(628−607 nm) = 10.8 $mM^{-1}$ $cm^{-1}$ (*31*). The concentration of the wild-type cytochrome *bd* was determined from the reduced *minus* as isolated difference spectrum, using $\Delta\epsilon$(560−580 nm) = 21.4 $mM^{-1}$ $cm^{-1}$ (*32*). The concentration of the E445A mutant protein was determined by the BCA assay using wild-type cytochrome *bd* as standard. Each of the measurements was repeated at least three times.

*EPR Spectroscopic Measurements*. X-band EPR spectra were acquired on a Bruker ESP 300 equipped with an Oxford liquid helium cryostat and ITC4 temperature controller. Spectra were recorded with ferricyanide-oxidized samples of both wild-type and mutant cytochrome *bd* at about 100 $\mu$M enzyme at 9 and 25 K.

*Resonance Raman Spectroscopy*. The enzyme concentrations of wild-type and E445A mutant cytochrome *bd* used for resonance Raman experiments were the same as for the EPR measurements. The reduction to the ferrous state was achieved by adding microliter aliquots of a 10 mM sodium dithionite solution to an argon-purged sample in the Raman capillary cell, and the reduction was monitored by UV−vis spectroscopy in the same cell. Resonance Raman spectra were obtained on a custom McPherson 2061/207 spectrograph (set at 0.67 m with variable gratings) equipped with a Princeton Instruments liquid nitrogen cooled CCD detector (LN-1100PB). Kaiser Optical supernotch filters were utilized to attenuate Rayleigh scattering. Excitation sources consisted of an Innova 302 krypton laser (413 nm) and a Liconix 4240NB He/Cd laser (442 nm). Spectra were collected in a 90 °C scattering geometry on samples at room temperature with a collection time of a few minutes. Frequencies were calibrated relative to indene and $CCl_4$ standards and were accurate to ±1 $cm^{-1}$. $CCl_4$ was also used to check the polarization conditions. Optical absorption spectra of the Raman samples were obtained on a Perkin-Elmer Lambda 9 spectrophotometer to monitor the samples before and after laser illumination.

*Redox Titrations*. Both wild-type and E445A mutant cytochrome *bd* samples were prepared as described above. The redox titration was carried out using the ultrathin layer spectroelectrochemical cell for the UV−vis as previously described (*33*, *34*) and kindly provided by Dr. Werner Mäntele (University of Frankfurt, Germany). The gold-grid working electrode was chemically modified by 2 mM cysteamine solution as reported before (*35*). To accelerate the redox reaction, 15 different mediators were added as reported in ref *35* to a total concentration of 40 $\mu$M each. At this concentration and with the path length below 10 $\mu$m, no spectral contributions from the mediators in the visible region could be detected in the control experiment with samples lacking the protein. As a supporting electrolyte, 100 mM KCl was added. Approximately 6−8 $\mu$L of protein sample was added, sufficient to fill the spectroelectrochemical cell. Changes in the absorption spectrum were monitored using a UVPC-2101 spectrophotometer (Shimadzu). The equilibration time was less than 10 min under the conditions as described above. Redox titrations were performed by stepwise setting the potential and recording the absorption spectrum after sufficient equilibration. All measurements were obtained at 5 °C and were repeated at least twice. Absorbance changes at 628 nm vs solution potential were used for generating the heme *d* titration curve, and both 428 and 560 nm were used for generating the heme *b* titration curve. The midpoint potentials ($E_m$) were obtained by interactive fitting to the Nernst equation, examining fits with 1, 2, or 3 $n = 1$ components, using the program Origin 5.0 (Microcal Software Inc.).

*Ubiquinol-1 Reduction of Cytochrome bd*. For the anaerobic reduction by ubiquinol, purified E445A was made anaerobic by purging with argon gas for 1 h in an anaerobic cuvette. Then a mixture of dithiothreitol and ubiquinone-1 was injected into the cuvette to final concentrations of 4 and 1 mM, respectively. A series of absorbance spectra were taken with the DW2000 spectrophotometer (Aminco) until no further changes could be observed. For the aerobic reduction, the same procedure was used, except the argon gas purge was omitted.

*FTIR Measurement of Cyanide Bound to Cytochrome bd*. Purified E445A (22 $\mu$M) was incubated in the presence of cyanide [50 mM sodium phosphate buffer, pH 7.6, 5 mM EDTA, 0.05% *N*-lauroylsarcosine (sodium salt), 25 mM potassium cyanide] for 2−3 h and then concentrated in a microconcentrator (Amicon, cutoff MW 50 kDa) by centrifugation. The sample was transferred to the electrochemical cell (*36*). The difference spectrum was measured for a step from −500 to 500 mV (against a Ag/AgCl reference electrode). Single beam spectra were recorded on a Bio-Rad 575C FTIR spectrophotometer at 5 °C after sufficient equilibration of the sample at the chosen potential. Typically, 320 interferograms at 4 $cm^{-1}$ resolution were added. Five to 10 spectra were then averaged to improve the signal-to-noise ratio.

## RESULTS

*Heme Analysis and Optical Spectra*. Some of the properties of the mutants are summarized in Table 1. Aside from the Q449A mutant, all of the mutants failed to support aerobic growth (no complementation in a genetic screening) and had

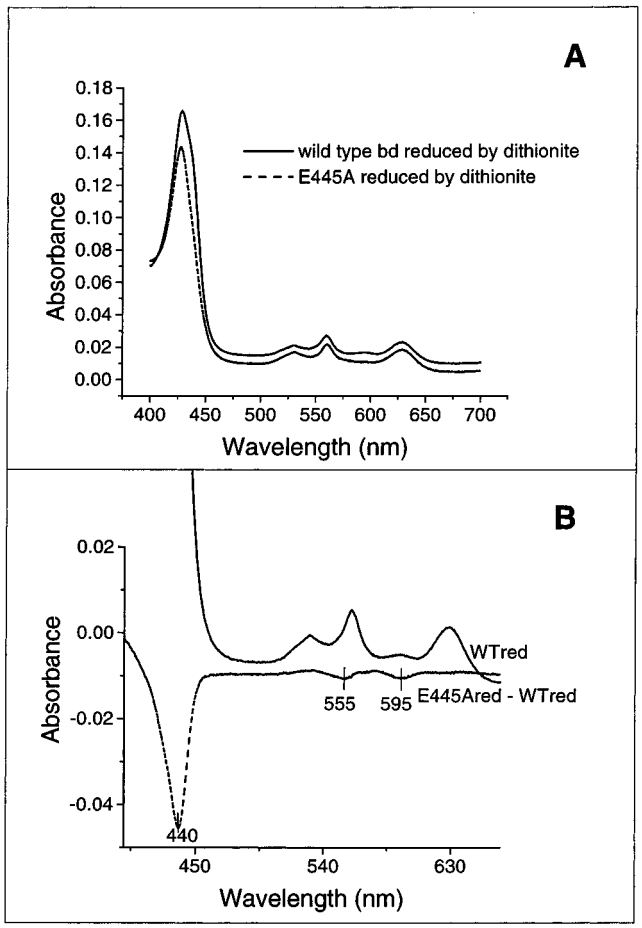


FIGURE 2: UV-vis absorbance spectra of wild-type and E445A mutant cytochrome *bd*. (A) Absolute spectra of the dithionite-reduced wild type (—) and E445A mutant (- - -) normalized to the same protein concentration. Conditions were as described in the Materials and Methods. (B) Dithionite-reduced E445A *minus* dithionite-reduced wild-type difference absorbance spectrum (- - -). The spectra used to generate the difference spectrum are the same as in panel A. The absolute dithionite-reduced spectrum of the wild type (—) is also shown in panel B for comparison.

little or no catalytic activity. The two mutants at position E445 (E445A and E445Q) appeared to be missing heme $b_{595}$, and E445A was selected for detailed analysis. The heme content of the E445A mutant was determined using the pyridine hemochromogen method and is close to one heme *b* per equivalent of enzyme, whereas the wild-type value is 2 (heme $b_{558}$ plus heme $b_{595}$). These results are consistent with the loss of one of the two *b*-type hemes in the enzyme (Table 1). The exact content of heme *b* of the isolated E445A mutant depends on the preparative protocol. Lower numbers (close to 1 per enzyme molecule) are obtained with preparations of the enzyme that use the conventional two-column purification protocol. It appears that one of the *b*-type hemes (heme $b_{595}$ as shown below) is destabilized by the mutation and that the extent of loss depends on the details of the preparation. In all cases, there is substantial loss of the heme, and in some preparations the loss appears to be complete.

The absolute spectrum (Figure 2A) of the dithionite-reduced E445A mutant indicates disappearance of the features associated with heme $b_{595}$, such as the α-band at 595 nm. There is also a substantial loss of absorbance in the Soret band. Spectroscopic properties of heme $b_{558}$ and heme *d* are not perturbed significantly, as evidenced by the visible part of the spectrum. The heme $b_{558}$ α- and β-band bands at 560 and 530 nm and the heme *d* near-IR band at 628 nm are present. The absence of the heme $b_{595}$ absorption bands can be better seen from the difference spectrum constructed by subtracting the wild-type spectrum from that of the mutant (E445A reduced minus wild-type reduced spectrum, Figure 2B). These spectra were normalized by the intensity of the heme *d* peak at 628 nm vs the 607 nm reference point. The difference spectrum has troughs at 595, 555, and 440 nm, which are all features expected for heme $b_{595}$ (*17*, *18*, *37*). These data show that the optical features of the reduced heme $b_{595}$ are missing in the mutant.

*EPR Spectra*. EPR spectra of the fully oxidized WT and E445A cytochrome *bd* were recorded at 9 and 20 K. The EPR spectrum of the oxidized WT cytochrome *bd* taken at 9 K is shown in Figure 3 and is essentially the same as described previously (*24*, *38*−*40*). In the low-field region (Figure 3B**)**, there are signals from high-spin heme(s) consisting of an axial component (features at $g = 6.07$ and 5.78) and a rhombic signal with the extrema at $g = 6.22$ and 5.66. The axial signal at $g = 6$ has been assigned earlier to heme *d* and the rhombic component to heme $b_{595}$ (*39*, *41*), although the opposite attribution has also been suggested in ref *40*. It is noted that the two hemes appear to be very close to each other, around 6 Å apart, and that they interact electronically (*17*), so the two hemes should have a strong mutual effect on their respective EPR signals.

In the high-field region (Figure 3B), there is a set of signals (features at $g = 2.50$, 2.40, 2.32, 1.86, and 1.83) previously assigned to a fraction of heme *d* which is low spin (*39*). The small positive peak at $g = 2.6$ has been previously attributed by Spinner et al. (*38*) to a detergent-induced modification of the enzyme. The low-spin heme $b_{558}$ has a so-called HALS ("highly anisotropic low spin") EPR spectrum, with $g_z$ around 3.5 (*38*). Notably, in the spectrum in Figure 3C, there are two peaks at $g = 3.67$ and 3.37. The broad trough at $g = 1.45$ has not previously been observed. This is probably the $g_x$ component of the $g \sim 3.5$ signal from heme $b_{558}$. The origin of the $g = 2.91$ signal, present in previously reported spectra, is also not known.

EPR spectra of the oxidized E445A mutant (normalized to the same concentration as the WT enzyme) show dramatic changes in the $g = 6$ region. Both the axial and rhombic signals seen of the WT enzyme are absent, replaced by a much broader, less intense signal. The most straightforward conclusion is that since heme $b_{595}$ is missing in the mutant, the remaining $g = 6$ signal belongs to high-spin heme *d*, which is altered compared to the signal in the WT enzyme. Part of the high-spin signal in the mutant may arise from a fraction of heme $b_{558}$ that has been converted to a high-spin form (*42*). Changes in the low-spin region of the spectrum are much smaller. The signals attributed to the low-spin heme *d* are almost identical with those observed with the WT enzyme. The EPR signal from the low-spin component of heme $b_{558}$ is affected by the E445A mutation. The relative amplitudes of the two components of the $g_z$ HALS signal from heme $b_{558}$ change in favor of the form with a peak at $g = 3.37$. Also, the trough at $g = 1.45$ shifts to $g = 1.67$ in the mutant. The mutation may shift the ratio of two conformations of the enzyme responsible for the two types of heme $b_{558}$ signals.

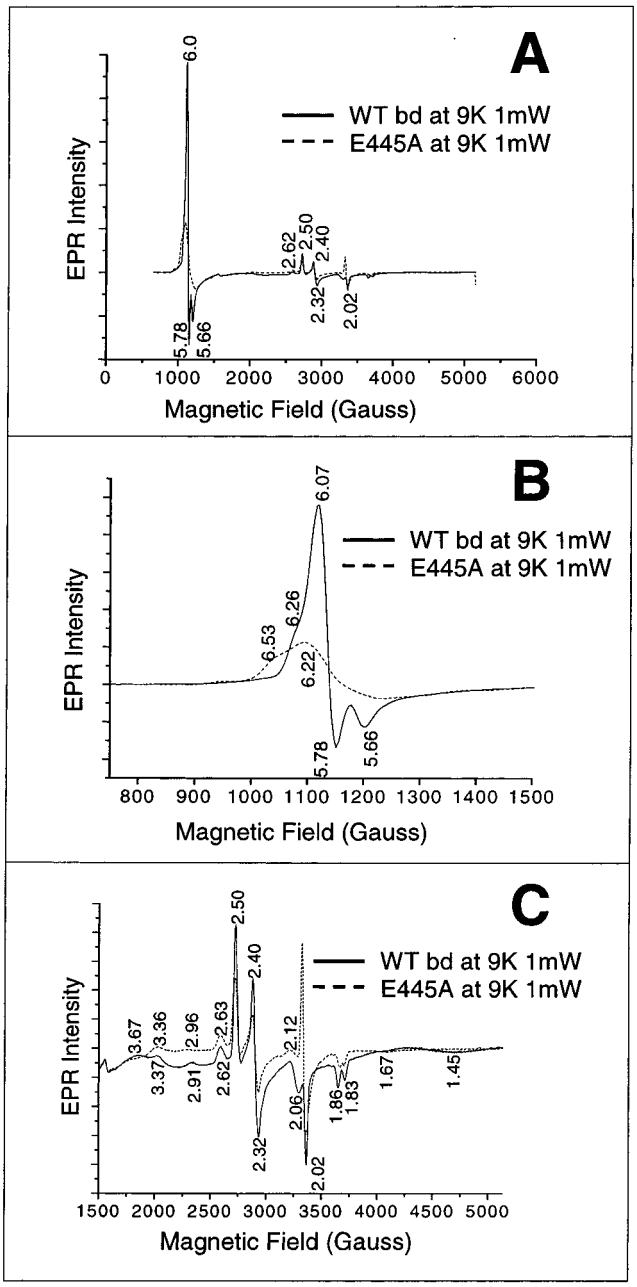


FIGURE 3: EPR spectra of the oxidized form of the wild-type and E445A mutant cytochrome *bd*. Wild-type enzyme (—) (100 $\mu$M) and E445A mutant (- - -) (86.5 $\mu$M) were preincubated with a mixture of mediators (5 $\mu$M each): DAD; 1,4-benzoquinone; 1,2-naphthoquinone-4-sulfonate. The samples were oxidized with ferricyanide (5 mM for at least 10 min under anaerobic conditions) and frozen in liquid nitrogen. Spectra were recorded at 9 K, 1 mW power, with a modulation frequency of 100 kHz and modulation amplitude of 32 G. The spectra have been normalized according to protein concentration. Panels B and C show expanded regions of the spectra. The numbers indicated in the figure are *g*-values.

*Resonance Raman Spectra*. High-frequency resonance Raman spectra of the fully reduced WT and E445A cytochrome *bd* oxidase were obtained with Soret excitation (Figure 4). Such resonance conditions have been shown to favor resonance Raman contributions of the heme $b_{595}$ of cytochrome *bd* oxidase (*43*). In the WT spectrum (Figure 4A), the characteristic high-spin $\nu_3$ at 1472 cm$^{-1}$ of ferrous heme $b_{595}$ is intense, while the $\nu_3$ of the low-spin ferrous heme $b_{558}$ at 1493 cm$^{-1}$ is weak. By comparison, the resonance Raman spectrum of the E445A mutant shows a

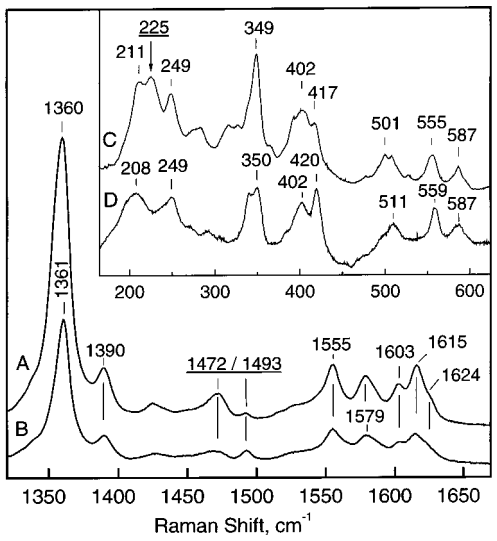


FIGURE 4: Resonance Raman spectra of reduced wild-type and E445A cytochrome *bd* oxidase: The high-frequency region of the WT (A) and E445A (B) resonance Raman spectra was obtained with a 413-nm excitation. The inset shows the low-frequency region of the WT (C) and E445A (B) resonance Raman spectra obtained with a 442-nm excitation.

significant decrease of the high-spin heme signal (Figure 4B). The loss of contributions assigned to the high-spin ferrous heme $b_{595}$ is also observed in the low-frequency resonance Raman spectra obtained with 442 nm excitation. The latter near-Soret excitation is known to selectively enhance iron−histidine stretching vibrations in ferrous high-spin heme species (*44*). In the WT spectrum a relatively strong band is observed at 225 cm$^{-1}$ (Figure 4C), but it is absent from the RR spectrum of the E445A mutant (Figure 4D). We assign this signal to the $\nu$(Fe−His) of ferrous heme $b_{595}$ and attribute its disappearance in the E445A mutant to the loss of $b_{595}$. This assignment is consistent with the ~1 cm$^{-1}$ upshift of this vibration in $^{54}$Fe-labeled WT cytochrome *bd* oxidase (*43*). Another resonance Raman study has assigned a band at 250 cm$^{-1}$ to the $\nu$(Fe−His) of ferrous heme (*45*). However, as discussed in ref *43*, the latter frequency is more likely to involve pyrrole tilting modes that also show $^{54}$Fe isotope upshifts (*46*).

*Carbon Monoxide Binding to the E445A Mutant*. The binding of CO to the reduced wild-type cytochrome *bd* induces changes in the Soret region of the spectrum with a characteristic "W" shape with a double trough at about 425−430 and 443−445 nm (Figure 5A, insert) (*31*). This peculiar W-shaped trough is not observed in the case of the CO complex of mixed-valence (ferrous heme *d* and ferric hemes *b*) wild-type enzyme and has, therefore, been assigned as a spectral perturbation of ferrous heme $b_{595}$ induced by CO binding to ferrous heme *d* (*17*). In the E445A mutant, the W-shaped trough in the Soret region is absent, and there is a simple minimum in the difference spectrum, the position of which varied between 434 and 439 nm for different preparations (Figure 5A). This observation is consistent with the absence of heme $b_{595}$ in the mutant enzyme. In the visible, the CO difference spectrum of the E445A mutant shows spectral changes around 550 and 630 nm diagnostic of CO binding with heme *d*. A more detailed attribution of the CO-induced spectral changes based on the comparison of the optical absorption, CD, and MCD data will be described elsewhere (Aruyunyan et al., paper in preparation).

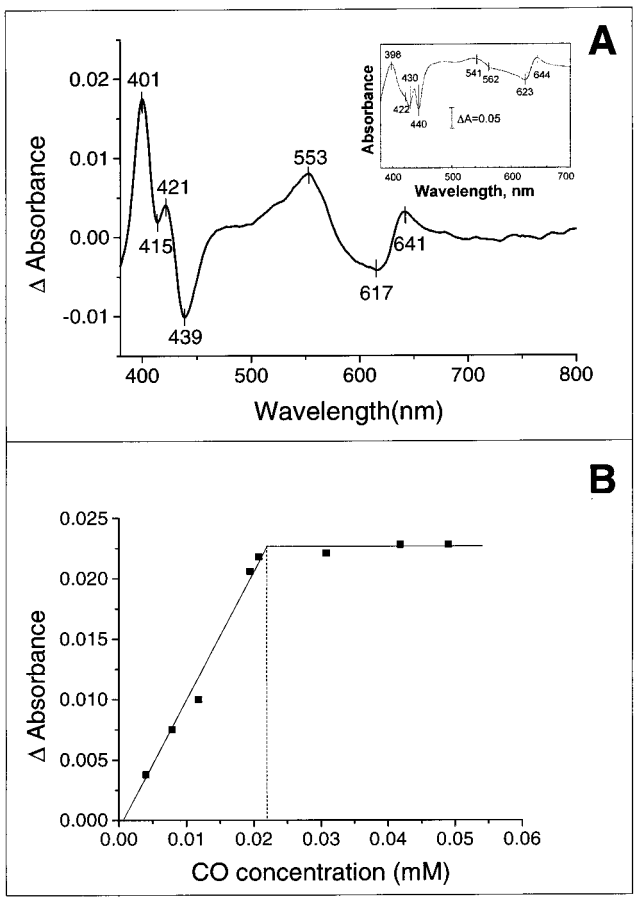


FIGURE 5: Reaction of the reduced E445A mutant cytochrome *bd* with CO. The E445A mutant (about 2.8 $\mu$M final concentration) was made anaerobic by purging argon gas for 1 h and was reduced by adding freshly made dithionite solution. The absorption spectrum was recorded and taken as a baseline. Aliquots of CO-saturated buffer were added to the sample, following which the absorbance spectra were taken. (A) A typical difference spectrum induced by addition of 25 $\mu$M CO. The insert shows the CO-induced difference spectrum obtained with the wild-type enzyme (from ref *31*). (B) The same protocol was followed for the CO titration except that the final protein concentration was about 21.2 $\mu$M. Absorbance changes at 642 nm minus 619 nm have been used to monitor CO binding to heme *d*.

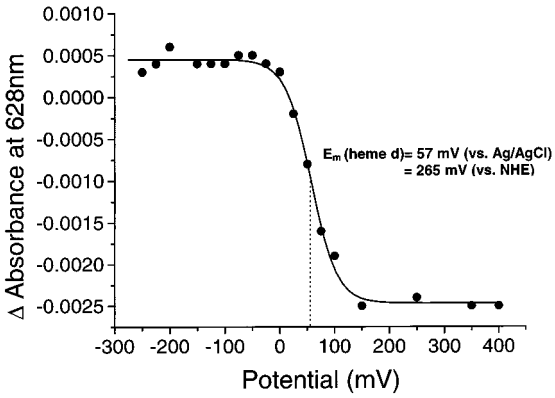


FIGURE 6: Redox titration of heme *d* in the E445A mutant. Oxidation−reduction of the hemes in the course of the titration was followed by recording the absorption spectra in the 400−700 nm region on a UVPC-2101 spectrophotometer (Shimadzu). The absorbance spectrum of the oxidized E445A sample (about 80 $\mu$M) was used as baseline. Redox-dependent absorbance changes at 628 nm were used to generate the data shown. *X*-axis values give the redox potential vs a Ag/AgCl electrode. See Materials and Methods for the description of the instrumentation and curve fitting protocol.

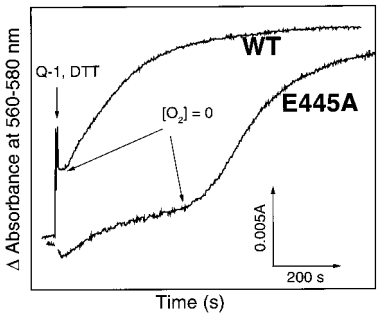


FIGURE 7: Kinetic traces of ubiquinol-1 reduction of the heme *b* component of cytochrome *bd* recorded under aerobic conditions. Ubiquinol-1 reduction of the wild-type and E445A mutant cytochrome *bd*. Measurements were recorded with a DW2000 spectrophotometer (SLM-Aminco). The reaction was initiated by adding a mixture of ubiquinol-1 and DTT (preincubated on ice for 30 min to fully reduce ubiquinone-1) to final concentrations of 220 $\mu$M and 1.1 mM, respectively. Both traces were normalized to the same heme *d* concentration. The final concentration was 0.66 $\mu$M for wild-type cytochrome *bd* and 0.44 $\mu$M for the E445A mutant.

A titration with CO was performed with the reduced E445A mutant, showing that the spectroscopic changes are linear with added CO until a clear titration end point (Figure 5B). Assuming that CO binds stoichiometrically to heme *d*, the titration yields a concentration of heme *d* of 21.6 $\mu$M in the sample, which is essentially the same value obtained independently by the reduced minus oxidized spectrum (21.2 $\mu$M). These data indicate that the E445A mutant has the full complement of heme *d*.

*Electrochemical Measurements*. The electrochemical titration of the E445A mutant (Figure 6) revealed that the heme *d* midpoint potential is the same as in the wild type (about 250 mV vs NHE). The titration of *b*-type hemes (monitored at 560 nm) (not shown) was biphasic for both the WT and E445A mutant. The major component has a midpoint potential of about 80 mV in both cases. This value depends on the detergent and other solution conditions (*47*) and is similar to previous measurements (*37*). Quantitation was not as clear due to apparent multiple components, which can be due to heme $b_{595}$ in the WT enzyme and, possibly, heterogeneity in heme $b_{558}$ in the mutant. Nevertheless, it can be concluded that the E445A mutation and the loss of heme $b_{595}$ have no major influence on the redox behavior of the two remaining hemes.

*Ubiquinol/TMPD Oxidase Activities*. The ubiquinol-1 oxidase activity is almost totally lost in the E445A mutant enzyme (less than 1% of that of the wild type). The same is found also for the TMPD oxidase activity (Table 1). In the presence of ubiquinol-1 under either aerobic or anaerobic conditions, the hemes of the E445A mutant eventually become reduced, characterized by the peaks of 562 nm from ferrous heme *b* and 628 nm of ferrous heme *d*. A comparison between the WT and mutant enzymes of the rates of aerobic reduction of the *b*-type hemes by ubiquinol is shown in Figure 7. Aerobic reduction of the wild-type enzyme with excess ubiquinol-1 occurs after the utilization of all the dioxygen. This is monitored using the wavelength pair of 560/580 nm (Figure 7) for the *b*-type hemes or 627/607 nm (data not shown) for heme *d*. There is a short (few seconds) apparent aerobic steady state in which the absorbance indicates about 30% reduction of the *b*-type hemes. Once dioxygen has been depleted, the rate of reduction of the

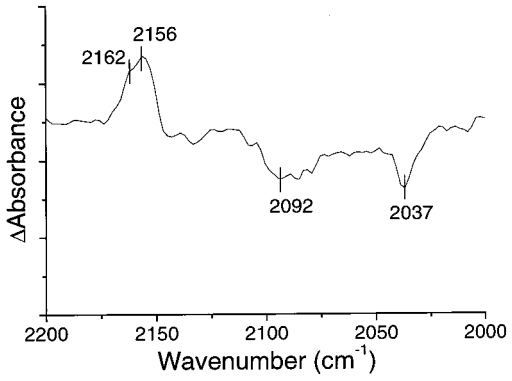


FIGURE 8: FTIR oxidized *minus* reduced difference spectrum of the cyanide-bound E445A mutant. The spectrum was recorded on a Bio-Rad 575C FTIR spectrophotometer (see Materials and Method for details). KCN was added to the sample buffer to a final concentration of 25 mM. The E445A protein sample (22 $\mu$M) was incubated in the above buffer for 2−3 h before measurement.

hemes is slow due to the fact that ubiquinol-1 is a rather weak reductant. The reduction of all three hemes proceeds simultaneously after anaerobiosis, so no internal electron transfer is rate limiting.

The kinetic trace is very different for the E445A mutant enzyme, as shown in Figure 7. One would expect heme $b_{558}$ to be fully reduced during the aerobic steady state if the mutation in E445A selectively perturbs the reaction of dioxygen at the heme *d* site, but this is not what is observed. Instead, there is a long lag phase, presumably reflecting the aerobic steady state during the very slow depletion of dioxygen from the buffer. Approximately one-third of heme $b_{558}$ is reduced during this phase, and heme *d* remains oxidized. Once oxygen is depleted (Figure 7), the reduction of heme $b_{558}$ (and heme *d*, not shown) proceeds. The rate of heme reduction after anaerobiosis is similar to that observed with the WT enzyme and presumably reflects the fact that quinol is not a potent reductant in the absence of the dioxygen electron acceptor.

The major observation is that of the initial aerobic steady-state spectrum if E445A does not display fully reduced heme $b_{558}$. It can be concluded that the E445 mutation does not simply block the reaction with dioxygen but appears also to impede the entry of electrons to heme $b_{558}$.

*FTIR Oxidized Minus Reduced Difference Spectrum of Cyanide Bound to Cytochrome bd*. The FTIR redox difference spectrum shown in Figure 8 is the enlarged view of the region characteristic for the C≡N vibrational mode. Spectra of the wild-type enzyme bound to cyanide have been reported, with a peak at 2161 $cm^{-1}$ for the oxidized enzyme, 2138 $cm^{-1}$ for the partially reduced enzyme (*24*, *32*), and 2084 $cm^{-1}$ for the photoreduced enzyme (*48*). The signal at 2161 $cm^{-1}$ was interpreted to indicate that cyanide can bridge the two high-spin hemes *d* and $b_{595}$ (*32*). In the E445A mutant, there is a new feature at 2156 $cm^{-1}$ of unknown origin which overlaps a band at 2162 $cm^{-1}$, thus making the latter a shoulder instead of a distinct peak. Nevertheless, the signal at 2162 $cm^{-1}$, presumably equivalent to the previously reported band at 2161 $cm^{-1}$ (*32*), appears to be present. The difference spectrum (Figure 8) also has a broad trough at approximately 2092 $cm^{-1}$ in the spectral range characteristic of free cyanide, due to the release of cyanide upon reduction of the enzyme, as previously reported (*32*, *48*). A trough due to cyanide bound to the ferrous heme iron in the fully reduced form of the mutant is observed at 2037 $cm^{-1}$. This mode was not previously reported for cytochrome *bd* in refs *32* and *48*. However, the spectra presented in the current work are based on electrochemical reduction of the enzyme, in which a lower potential can be achieved to fully reduce the enzyme. The previous report of cyanide bound to the photoreduced enzyme described a band at 2084 $cm^{-1}$ (*48*).

## DISCUSSION

The cytochrome *bd* quinol oxidase is found in many prokaryotes and is often associated with microaerophilic growth conditions (*2*−*4*). Although not a proton pump, the enzyme is electrogenic (*7*, *49*), so that quinol oxidation results in charge separation across the membrane. The mechanism by which the enzyme generates a protonmotive force is of interest. Almost certainly, the charge separation results from the fact that electrons and protons that are used to reduce dioxygen to water originate from opposite sides of the membrane (*7*, *8*, *37*, *49*−*51*). Specific residues required for quinol binding have not been identified, but it is known that quinol oxidation involves the "Q-loop" (*52*−*55*), which is a hydrophilic loop connecting transmembrane helices 6 and 7 in subunit I, and is on the periplasmic side of the membrane (*56*). The low-spin heme $b_{558}$ component that is thought to be the initial electron acceptor from quinol (*16*) is ligated to His186 (*57*) and Met393 (*25*, *38*), also located near the periplasmic surface of subunit I (*20*). The dioxygen binding site is heme *d* (*18*, *19*), which has not been localized with respect to the membrane bilayer. However, it appears that heme *d* shares the same binding pocket within the protein with heme $b_{595}$ (*17*, *22*), which is ligated to His19 in subunit I (*43*). Recently, the predicted topology of subunit I was revised such that His19 is now also predicted to be near the periplasmic surface (*20*).

The work presented here shows that E445, located within a highly conserved region in subunit I, is required to stabilize the binding of heme $b_{595}$. Since the region of the protein containing E445 is located on the periplasmic side of the membrane, it is reasonable to conclude that the heme $b_{595}$−heme *d* binuclear center is located near the periplasm. Since the protons used to form water must originate from the bacterial cytoplasm, the enzyme must provide a proton-conducting pathway for protons to reach the dioxygen reactive site near the opposite side of the membrane. This situation is very similar to that of the heme−copper oxidases, where proton pathways leading to the binuclear center have been well characterized (*58*).

The purified E445A mutant is remarkable insofar as it is lacking one of the three heme prosthetic groups and yet appears to be otherwise intact, albeit nonfunctional. The amount of protein that is expressed in *E. coli* is substantially less than in the wild-type enzyme, but the isolated mutant is stable. The absence of heme $b_{595}$ in the membranes containing the mutant enzyme is apparent from the lack of the characteristic peak at 595 nm in the reduced minus oxidized difference spectrum (not shown), and this is confirmed in the isolated enzyme. All of the spectroscopic and analytical techniques indicate the absence of heme $b_{595}$ in the E445A mutant. It is remarkable that the redox midpoint potential

and spectral characteristics of heme *d* appear to be undisturbed by the loss of heme $b_{595}$, despite the fact that these two hemes appear to be physically close and within the same protein binding pocket (*17*, *22*). The low-spin heme $b_{558}$ appears, however, to be somewhat perturbed by the mutation.

The loss of heme $b_{595}$ results in changes in the UV−vis absorption spectra consistent with previous spectroscopic assignments (*17*, *18*, *37*) and confirms these assignments. The resonance Raman spectrum of the E445A mutant also confirms the assignment of the band at 225 $cm^{-1}$ as the ferrous iron−histidine stretching frequency for heme $b_{595}$ (*43*).

The FTIR redox difference spectrum of cyanide bound to the enzyme is less affected by the mutation than expected. The band at 2162 $cm^{-1}$ appears to be present, although as a shoulder on a new feature at 2156 $cm^{-1}$ (Figure 8). Previously, the 2162 $cm^{-1}$ band was tentatively assigned as being due to cyanide bridging between heme *d* and heme $b_{595}$ (*24*, *32*). The current data suggest that this may not be correct, since the band is still present in the E445A mutant in which heme $b_{595}$ is absent. Possibly, the 2162 and 2156 $cm^{-1}$ bands represent different conformers of the cyanide complex of the oxidized cytochrome *bd* mutant, strongly influenced by interactions between the cyanide moiety and protein residue(s). An alternate explanation of the current data is that the preparation of the mutant used for the FTIR experiments contained sufficient residual heme $b_{595}$ to yield the observed band at 2162 $cm^{-1}$, but this is unlikely. Further study of this issue is warranted since the presence of a bridged cyanide between heme *d* and heme $b_{595}$ places severe structural contraints on the distance between the heme irons.

The absence of heme $b_{595}$ results in loss of catalytic function, using either ubiquinol-1 or TMPD as reductant. Heme $b_{595}$ and heme *d* are known to be physically close and appear to function as a diheme unit (*22*), and heme $b_{595}$ is required for rapid electron transfer between heme $b_{558}$ and heme *d* (*59*). Therefore, it might be expected that the loss of heme $b_{595}$ would specifically block the reaction with dioxygen or the electron transfer between heme $b_{558}$ and heme *d*. However, the loss of function of the E445A mutant cannot be uniquely ascribed to a block of processes following the reduction of heme $b_{558}$ since inhibition of these steps would result in full reduction of heme $b_{558}$ during the aerobic steady state, and this is not observed. Both the reduction of heme $b_{558}$ and the reoxidation of heme $b_{558}$ must be inhibited by the E445A mutation, presumably due to the loss of heme $b_{595}$.

The current work indicates not only that the site of quinol oxidation and the dioxygen reactive site are on the same side of the membrane but that they are likely to be relatively close to each other.

## ACKNOWLEDGMENT

We gratefully thank Jeffrey Sigman for helping with the EPR measurement, Dr. Vitaliy Borisov, Dr. Blanca Barquera, Dr. Charles Scholes, and Dr. Graham Palmer for fruitful discussions, and Eric Johnson at the UIUC Fermentation Facility for cell growth.

## REFERENCES

1. Anraku, Y., and Gennis, R. B. (1987) *Trends Biochem. Sci. 12*, 262−266.
2. Rice, C. W., and Hempfling, W. P. (1978) *J. Bacteriol. 134*, 115−124.
3. Fu, H.-A., Iuchi, S., and Lin, E. C. C. (1991) *Mol. Gen. Genet. 226*, 209−213.
4. Cotter, P. A., Chepuri, V., Gennis, R. B., and Gunsalus, R. P. (1990) *J. Bacteriol. 172*, 6333−6338.
5. Miller, M. J., and Gennis, R. B. (1983) *J. Biol. Chem. 258*, 9159−9165.
6. Green, N. G., Fang, H., Lin, R.-J., Newton, G., Mather, M., Georgiou, C., and Gennis, R. B. (1988) *J. Biol. Chem. 263*, 13138−13143.
7. Miller, M. J., and Gennis, R. B. (1985) *J. Biol. Chem. 260*, 14003−14008.
8. Miller, M. J., and Gennis, R. B. (1986) *Methods Enzymol. 126*, 138−145.
9. Gennis, R. B. (1987) *FEMS Microbiol. Rev. 46*, 387−399.
10. Jünemann, S. (1997) *Biochim. Biophys. Acta 1321*, 107−127.
11. Mogi, T., Tsubaki, M., Hori, H., Miyoshi, H., Nakamura, H., and Anraku, Y. (1998) *J. Biochem. Mol. Biol. Biophys. 2*, 79−110.
12. Calhoun, M. W., Thomas, J. W., and Gennis, R. B. (1994) *Trends Biochem. Sci. 19*, 325−330.
13. Garcia-Horsman, J. A., Barquera, B., Rumbley, J., Ma, J., and Gennis, R. B. (1994) *J. Bacteriol. 176*, 5587−5600.
14. Puustinen, A., Finel, M., Haltia, T., Gennis, R. B., and Wikström, M. (1991) *Biochemistry 30*, 3936−3942.
15. Timkovich, R., Cork, M. S., Gennis, R. B., and Johnson, P. Y. (1985) *J. Am. Chem. Soc. 107*, 6069−6075.
16. Green, G. N., Lorence, R. M., and Gennis, R. B. (1986) *Biochemistry 25*, 2309−2314.
17. Vos, M. H., Borisov, V. B., Liebl, U., Martin, J.-L., and Konstantinov, A. A. (2000) *Proc. Natl. Acad. Sci. U.S.A. 97*, 1554−1559.
18. Hori, H., Tsubaki, M., Mogi, T., and Anraku, Y. (1996) *J. Biol. Chem. 271*, 9254−9258.
19. Hill, S., Viollet, S., Smith, A. T., and Anthony, C. (1990) *J. Bacteriol. 172*, 2071−2078.
20. Osborne, J. P., and Gennis, R. B. (1999) *Biochim. Biophys. Acta 1410*, 32−50.
21. Hata-Tanaka, A., Matsuura, K., Itoh, S., and Anraku, Y. (1987) *Biochim. Biophys. Acta 893*, 289−295.
22. Hill, J. J., Alben, J. O., and Gennis, R. B. (1993) *Proc. Natl. Acad. Sci. U.S.A. 90*, 5863−5867.
23. D'mello, R., Palmer, S., Hill, S., and Poole, R. K. (1994) *FEMS Microbiol. Lett. 121*, 115−120.
24. Tsubaki, M., Mogi, T., and Hori, H. (1999) *J. Biochem. 126*, 510−519.
25. Kaysser, T. M., Ghaim, J. B., Georgiou, C., and Gennis, R. B. (1995) *Biochemistry 34*, 13491−13501.
26. Dassa, J., Fsihi, H., Marck, C., Dion, M., Kieffer-Bontemps, M., and Boquet, P. L. (1991) *Mol. Gen. Genet. 229*, 341−352.
27. Osborne, J. (1999), Ph.D. Thesis, University of Illinois.
28. Chung, C. T., Niemela, S. L., and Miller, R. H. (1989) *Proc. Natl. Acad. Sci. U.S.A. 86*, 2172−2175.
29. Cohen, G. N., and Rickenberg, H. V. (1956) *Ann. Inst. Pasteur (Paris) 91*, 693−720.
30. Berry, E. A., and Trumpower, B. L. (1987) *Anal. Biochem. 161*, 1−15.
31. Borisov, V., Arutyunyan, A. M., Osborne, J. P., Gennis, R. B., and Konstantinov, A. A. (1999) *Biochemistry 38*, 740−750.
32. Tsubaki, M., Hori, H., Mogi, T., and Anraku, Y. (1995) *J. Biol. Chem. 270*, 28565−28569.
33. Moss, D., Nabedryk, E., Breton, J., and Mäntele, W. (1990) *Eur. J. Biochem. 187*, 565−572.
34. Mantele, W. (1996) in *Biophysical Techniques in Photosynthesis*, Kluwer, Dordrecht, The Netherlands.
35. Hellwig, P., Behr, J., Ostermeier, C., Richter, O.-M. H., Pfitzner, U., Odenwald, A., Ludwig, B., Michel, H., and Mäntele, W. (1998) *Biochemistry 37*, 7390−7399.
36. Mantele, W. (1993) *Trends Biochem. Sci. 18*, 197−202.
37. Koland, J. G., Miller, M. J., and Gennis, R. B. (1984) *Biochemistry 23*, 1051−1056.

38. Spinner, F., Cheesman, M. R., Thomson, A. J., Kaysser, T., Gennis, R. B., Peng, Q., and Peterson, J. (1995) *Biochem. J. 308*, 641−644.
39. Meinhardt, S. W., Gennis, R. B., and Ohnishi, T. (1989) *Biochim. Biophys. Acta 975*, 175−184.
40. Tsubaki, M., Mogi, T., and Hori, H. (1999) *J. Biochem. 126*, 98−103.
41. Rothery, R., and Ingledew, W. J. (1989) *Biochem. J. 262*, 437−443.
42. Hata, A., Kirino, Y., Matsuura, K., Itoh, S., Hiyama, T., Konishi, K., Kita, K., and Anraku, Y. (1985) *Biochim. Biophys. Acta 810*, 62−72.
43. Sun, J., Kahlow, M. A., Kaysser, T. M., Osborne, J. P., Hill, J. J., Rohlfs, R. J., Hille, R., Gennis, R. B., and Loehr, T. M. (1996) *Biochemistry 35*, 2403−2412.
44. Kitagawa, T. (1987) *Biological Applications of Raman Spectroscopy* (Spiro, T. G., Ed.) Vol. III, pp 97−131, John Wiley & Sons, New York.
45. Hirota, S., Mogi, T., Anraku, Y., Gennis, R. B., and Kitagawa, T. (1995) *Biospectroscopy 1*, 305−311.
46. Choi, S., Lee, J. J., Wei, Y. H., and Spiro, T. G. (1983) *J. Am. Chem. Soc. 105*, 3692−3707.
47. Lorence, R. M., Green, G. N., and Gennis, R. B. (1984) *J. Bacteriol. 157*, 115−121.
48. Yamazaki, Y., Kandori, H., and Mogi, T. (1999) *J. Biochem. 125*, 1131−1136.
49. Jasaitis, A., Borisov, V. B., Belevich, N. P., Morgan, J. E., Konstantinov, A. A., and Verkhovsky, M. I. (2000) *Biochemistry 39*, 13800−13809.
50. Minghetti, K. C., and Gennis, R. B. (1988) *Biochem. Biophys. Res. Commun. 155*, 243−248.
51. Kita, K., Konishi, K., and Anraku, Y. (1984) *J. Biol. Chem. 259*, 3375−3381.
52. Kranz, R. G., and Gennis, R. B. (1984) *J. Biol. Chem. 259*, 7998−8003.
53. Dueweke, T. J., and Gennis, R. B. (1990) *J. Biol. Chem. 265*, 4273−4277.
54. Dueweke, T. J., and Gennis, R. B. (1991) *Biochemistry 30*, 3401−3406.
55. Yang, F.-D., Yu, L., Yu, C.-A., Lorence, R. M., and Gennis, R. B. (1986) *J. Biol. Chem. 261*, 14987.
56. Ghaim, J. B., Greiner, D. P., Meares, C. F., and Gennis, R. B. (1995) *Biochemistry 34*, 11311−11315.
57. Fang, H., Lin, R.-J., and Gennis, R. B. (1989) *J. Biol. Chem. 264*, 8026−8032.
58. Gennis, R. B. (1998) *Biochim. Biophys. Acta 1365*, 241−248.
59. Kobayashi, K., Tagawa, S., and Mogi, T. (1999) *Biochemistry 38*, 5913−5917.

BI010469M